J|A|C|S

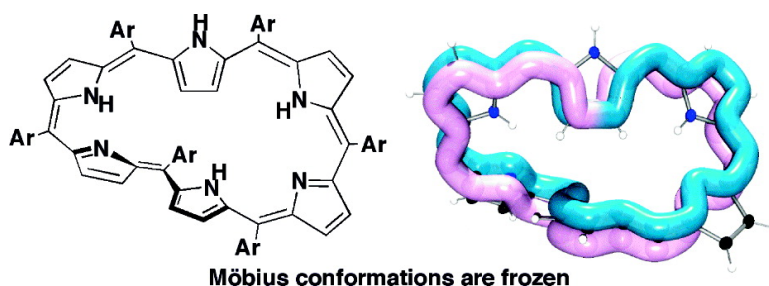## JOURNAL OF THE AMERICAN CHEMICAL SOCIETY

Article

Unambiguous Identification of Mo#bius Aromaticity
for *meso*-Aryl-Substituted [28]Hexaphyrins(1.1.1.1.1.1)

Jeyaraman Sankar, Shigeki Mori, Shohei Saito, Harapriya Rath, Masaaki Suzuki, Yasuhide Inokuma,
Hiroshi Shinokubo, Kil Suk Kim, Zin Seok Yoon, Jae-Yoon Shin, Jong Min Lim, Yoichi Matsuzaki,
Osamu Matsushita, Atsuya Muranaka, Nagao Kobayashi, Dongho Kim, and Atsuhiro Osuka

Möbius conformations are frozen

More About This Article

Additional resources and features associated with this article are available within the HTML version:

- Supporting Information
- Access to high resolution figures
- Links to articles and content related to this article
- Copyright permission to reproduce figures and/or text from this article

View the Full Text HTML

ACS Publications

High quality. High impact.

Unambiguous Identification of Möbius Aromaticity for meso-Aryl-Substituted [28]Hexaphyrins(1.1.1.1.1.1)

Jeyaraman Sankar,[†] Shigeki Mori,[†] Shohei Saito,[†] Harapriya Rath,[†]
Masaaki Suzuki,[†] Yasuhide Inokuma,[†] Hiroshi Shinokubo,[†] Kil Suk Kim,[‡]
Zin Seok Yoon,[‡] Jae-Yoon Shin,[‡] Jong Min Lim,[‡] Yoichi Matsuzaki,[ǁ]
Osamu Matsushita,[§] Atsuya Muranaka,[§] Nagao Kobayashi,*[,§] Dongho Kim,*[,‡] and
Atsuhiro Osuka*[,†]

*Department of Chemistry, Graduate School of Science, Kyoto University, Sakyo-ku,
Kyoto 606-8502, Japan, Center for Ultrafast Optical Characteristics Control and Department of
Chemistry, Yonsei University, Seoul 120-749, Korea, Department of Chemistry, Graduate School
of Science, Tohoku University, Aoba-ku, Sendai 980-8578, Japan, Advanced Technology
Research Laboratories, Nippon Steel Corporation, 20-1 Shintomi, Futtsu,
Chiba 293-8511, Japan*

Received March 17, 2008; E-mail: nagaok@mail.tains.tohoku.ac.jp; dongho@yonsei.ac.kr; osuka@kuchem.kyoto-u.ac.jp

Abstract: *meso*-Aryl-substituted [28]hexaphyrins(1.1.1.1.1.1) have been examined by ^{1}H, ^{13}C, and ^{19}F NMR spectroscopies, UV−vis absorption spectroscopy, magnetic circular dichroism spectroscopy, and single-crystal X-ray diffraction analysis. All of these data consistently indicate that [28]hexaphyrins(1.1.1.1.1.1) in solution at 25 °C exist largely as an equilibrium among several rapidly interconverting twisted Möbius conformations with distinct aromaticities, with a small contribution from a planar rectangular conformation with antiaromatic character at slightly higher energy. In the solid state, [28]hexaphyrins(1.1.1.1.1.1) take either planar or Möbius-twisted conformations, depending upon the *meso*-aryl substituents and crystallization conditions, indicating a small energy difference between the two conformers. Importantly, when the temperature is decreased to −100 °C in THF, these rapid interconversions among Möbius conformations are frozen, allowing the detection of a single [28]hexaphyrin(1.1.1.1.1.1) species having a Möbius conformation. Detailed analyses of the solid-state Möbius structures of compounds **2b**, **2c**, and **2f** showed that singly twisted structures are achieved without serious strain and that cyclic π-conjugation is well-preserved, as needed for exhibiting strong diatropic ring currents. Actually, the harmonic-oscillator model for aromaticity (HOMA) values of these structures are significantly large (0.85, 0.69, and 0.71, respectively), confirming the first demonstration of stable Möbius aromatic systems consisting of free-base expanded porphyrins without the assistance of metal coordination.

Introduction

The Hückel rule[1] that predicts aromaticity for [4n + 2]annulenes and antiaromaticity for [4n]annulenes lying in a plane has been the firm basis for understanding aromaticity. As a topological complement of the Hückel rule, the concept of Möbius aromaticity predicts that aromatic characteristics will appear for [4n]annulenes when they are lying on a twisted Möbius strip.[2] This important concept was first implied by Heilbronner[3] in 1964 and later proposed for transition states[4] and reactive intermediates[5] and extensively discussed in relation

to the Walsh model for cyclopropane.[6] These theoretical studies stimulated the synthesis of actual Möbius aromatic molecules, which had been elusive until the seminal work of Herges and co-workers,[7] who reported the synthesis of [16]annulene molecules having a twisted topology as the first examples of Möbius aromatic molecules; the synthesis was achieved by a strategic lateral combination of a normal planar conjugated segment and a belt-shaped conjugated segment. The aromatic characters of these macrocycles were argued with respect to the large dihedral angle (−107.7°) and small nucleus-independent chemical shift (NICS) value (−3.4 ppm).[8] However, Herges and co-workers[7b] showed that Möbius-twisted annulenes are

† Kyoto University.
‡ Yonsei University.
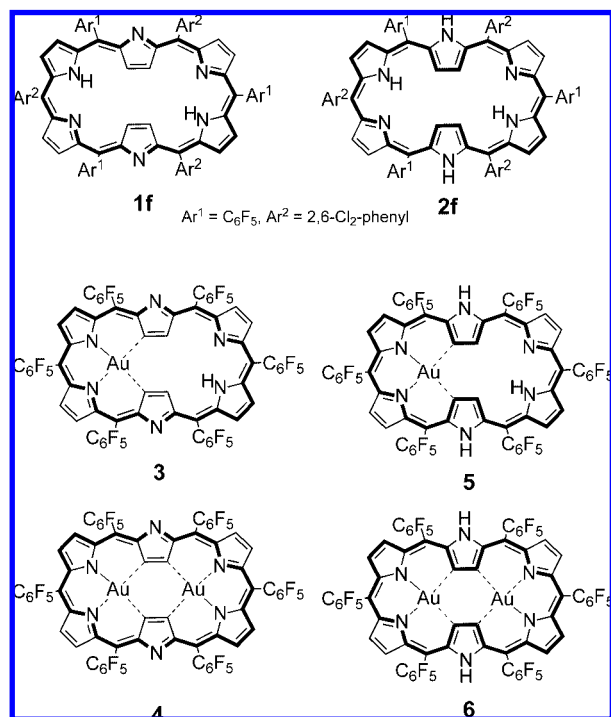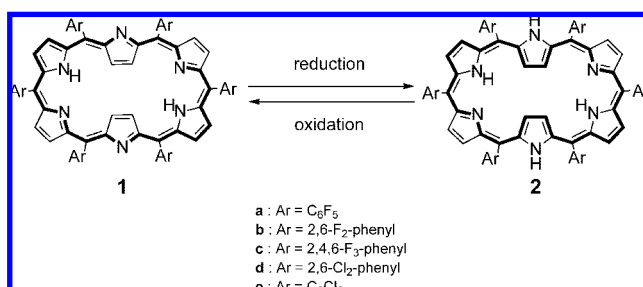ǁ Nippon Steel Corporation.
§ Tohoku University.

(1) (a) Hückel, E. *Z. Phys.* **1931**, *70*, 204–286. (b) Hückel, E. *Z. Phys.* **1932**, *76*, 628–648.
(2) (a) Rzepa, H. S. *Chem. Rev.* **2005**, *105*, 3697–3715. (b) Herges, R. *Chem. Rev.* **2006**, *106*, 4820–4842.
(3) Heilbronner, E. *Tetrahedron Lett.* **1964**, *5*, 1923–1926.
(4) Zimmerman, H. E. *J. Am. Chem. Soc.* **1966**, *88*, 1564–1567.
(5) Mauksch, M.; Gogonea, V.; Jiao, H.; Schleyer, P. v. R. *Angew. Chem., Int. Ed.* **1998**, *37*, 2395–2398.

(6) (a) The Walsh model for cyclopropane was first proposed in: Walsh, A. D. *Nature* **1947**, *159*, 165. (b) It was organized in: Walsh, A. D. *Trans. Faraday Soc.* **1949**, *45*, 179–190. (c) In this context, Zimmerman indicated that the p orbitals of the model could be treated as a Möbius circle, as well as those of barrelene and allene. See: Zimmerman, H. E. *Acc. Chem. Res.* **1971**, *4*, 272–280, and references therein.
(7) (a) Ajami, D.; Oeckler, O.; Simon, A.; Herges, R. *Nature* **2003**, *426*, 819–821. (b) Ajami, D.; Hess, K.; Köhler, F.; Näther, C.; Oeckler, O.; Simon, A.; Yamamoto, C.; Okamoto, Y.; Herges, R. *Chem.−Eur. J.* **2006**, *12*, 5434–5455.

Chart 1

$Ar^1 = C_6F_5$, $Ar^2 = $ 2,6-Cl$_2$-phenyl

Scheme 1

a : Ar = C$_6$F$_5$
b : Ar = 2,6-F$_2$-phenyl
c : Ar = 2,4,6-F$_3$-phenyl
d : Ar = 2,6-Cl$_2$-phenyl
e : Ar = C$_6$Cl$_5$

more aromatic than nontwisted isomers through the use of an extensive examination of all possible data following a principal-component analysis. A main difficulty in the synthesis of Möbius aromatic molecules lies in the need to compromise two conflicting structural elements, a twisting single-sided topology and a overall macrocyclic conjugation, with a $4n$ π-electron system. Möbius aromatic compounds must contain large annu-

lenic systems to mitigate distortion associated with a single molecular twist. In such a situation, however, cis−trans isomerization barriers would be very small, making it very difficult to lock-in a twisted structure. A recent interesting example is a di-*p*-benzihexaphyrin reported by Latos-Grażyński and co-workers[9] that exhibits a Möbius structure in the solid state but shows a temperature-dependent Hückel-to-Möbius topological switch in solution.

Because of their unique chemical and optical properties as well as their versatile coordination chemistry, increasing attention has recently been focused on expanded porphyrins that consist of more than five pyrrolic subunits.[10] Among these, we reported the synthesis of a series of *meso*-aryl-expanded porphyrins using a modified Rothemund−Lindsey protocol.[11] As one of their unique and surprising properties, [36]octaphyrin(1.1.1.1.1.1.1.1), [32]heptaphyrin(1.1.1.1.1.1.1), and [26]hexaphyrins(1.1.1.1.1.1) have been demonstrated to spontaneously provide stable Möbius aromatic molecules upon metalation with group-10 metals.[12] These are the first twisted Möbius molecules with distinct aromaticities, as indicated by their large differences between the chemical shifts of the outer and inner β-protons, large negative NICS values, and large two-photon absorption cross sections. Quite recently, we reported that a Möbius aromatic molecule was also formed from metalation of an N-fused pentaphyrin with a Rh(I) salt as the smallest Möbius structure from expanded porphyrins.[13] In these two cases, metal coordination plays a vital role in locking the structures into stable Möbius aromatic conformations. In contrast, none of the free-base expanded porphyrins reported to date has exhibited distinct Möbius aromaticity without any assistance from metal coordination.

meso-Hexakis(pentafluorophenyl)-substituted [26]hexaphyrin(1.1.1.1.1.1) (**1a**) is a planar rectangular macrocycle with a metallic luster in the solid state and a vivid purple color in solution.[11a,14] This expanded porphyrin can be regarded as a representative porphyrin homologue in terms of its planar structure and strong aromaticity. The ^{1}H NMR spectrum of **1a** reveals a distinct diatropic ring current by displaying strongly shielded signals due to the inner β- and NH-protons and strongly deshielded signals due to the outer β-protons. We recently reported that metalation of **1a** with Au(III) ion provided the almost-planar mono[Au(III)] and bis[Au(III)] complexes **3** and **4** (Chart 1), which have planar, conjugated structures with 26 π electrons and thus exhibit Hückel aromaticity. Importantly, complexes **3** and **4** were reduced with NaBH$_4$ to the corresponding [28]hexaphyrins **5** and **6**
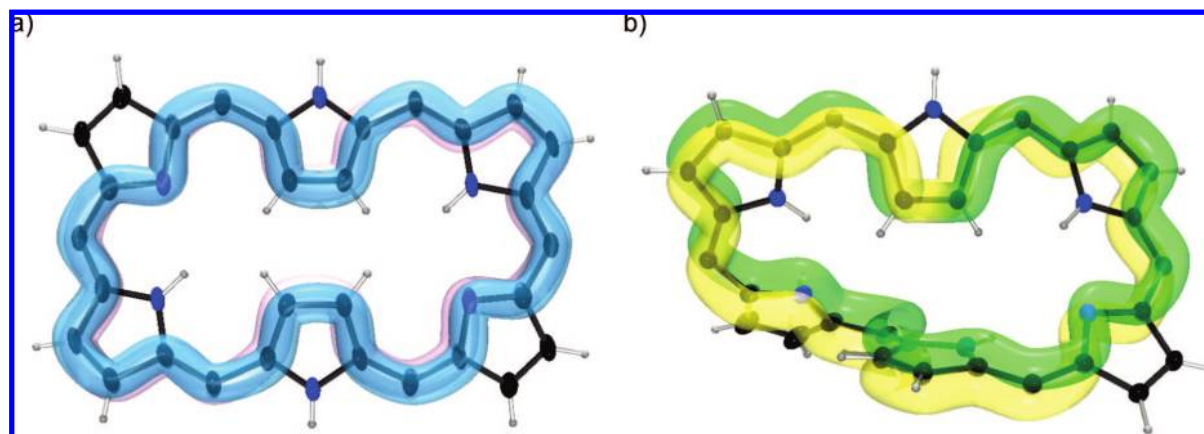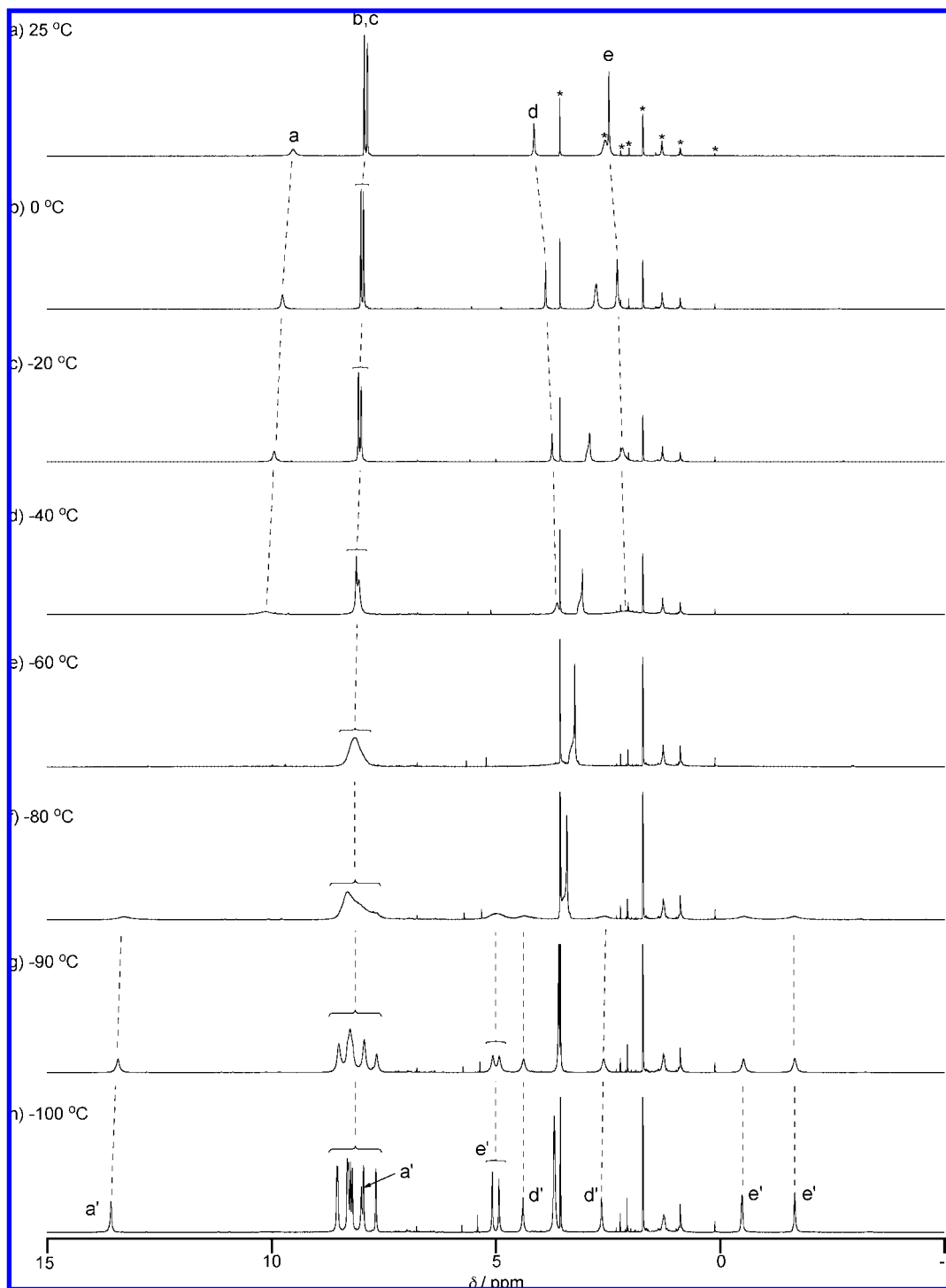

Figure 1. Topological models of [28]hexaphyrins: (a) planar rectangular conformation of Hückel topology; (b) twisted Möbius topology.

Figure 2. Variable-temperature ^{1}H NMR spectra of **2a** in THF-d_8 from 25 to −100 °C. Peaks marked with * are due to residual solvents and impurities.

(Chart 1), both of which display strong paratropic ring currents due to their planar, conjugated structures with 28 π electrons.[15] On the other hand, the structures and electronic natures of the *meso*-aryl-substituted [28]hexaphyrin(1.1.1.1.1.1) free bases **2** have been puzzling so far, since the ^{1}H NMR spectrum of **2a** seems to suggest that it has a symmetric planar rectangular conformation and a moderate diatropic ring

current, but such a planar conformation with 28 π electrons should lead to a paratropic ring current according to the Hückel rule (Figure 1a). This contradiction has been a big mystery since the discovery of **2** in 1999.[14]

In this paper, we demonstrate that the *meso*-aryl-substituted [28]hexaphyrin(1.1.1.1.1.1) free bases **2** are conformationally rather floppy molecules that in solution at room temperature

(8) Castro, C.; Chen, Z.; Wannere, C. S.; Jiao, H.; Karney, W. L.; Mauksch, M.; Puchta, R.; Hommes, N. J. R. v. E.; Schleyer, P. v. R. *J. Am. Chem. Soc.* **2005**, *127*, 2425–2432.

(9) Stepień, M.; Latos-Grażyński, L.; Sprutta, N.; Chwalisz, P.; Szterenberg, L. *Angew. Chem., Int. Ed.* **2007**, *46*, 7869–7873.

Scheme 2. Plausible Conformational Changes of **2** in Solution Among **P** (Having a Planar Hückel Topology) and **M1**−**M4** (Having Twisted Möbius Topologies). For **2a**−**e**, **M1** is Identical to **M4** and **M2** is Identical to **M3**, and These Two Pairs are Enantiomeric. In the Case of **2f**, **M1** and **M4** are Enantiomers of Each Other, as are **M2** and **M3**
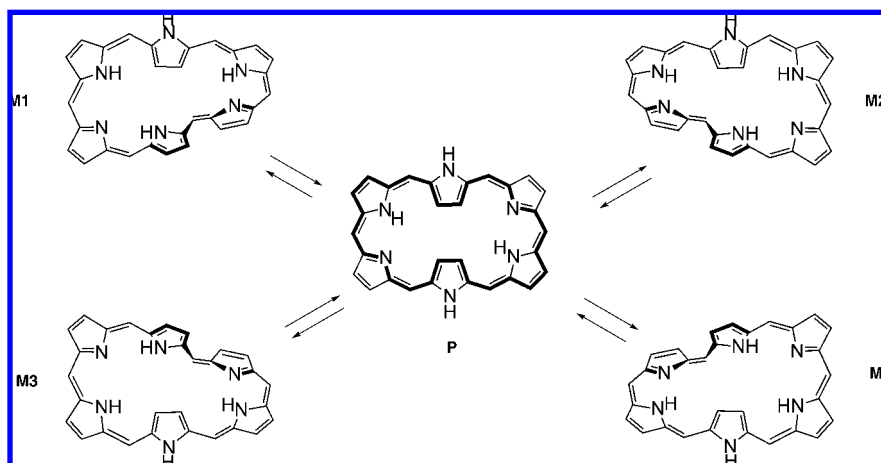
exist largely as an equilibrium among rapidly interconverting twisted Möbius structures with distinct aromaticities (Figure 1b).

Results and Discussion

NMR Measurements. [26]Hexaphyrins **1a**−**f** were prepared according to our reported methods[11c] and quantitatively reduced to the corresponding [28]hexaphyrins **2a**−**f** by NaBH$_4$ reduction (Scheme 1). Compounds **2a**−**f** display characteristic blue colors in solution. As shown in Figure 2a, the ^{1}H NMR spectrum of **2a** in THF-d_8 at 25 °C is simple, exhibiting a singlet at 2.46 ppm for four β-protons (signal e), a broad signal at 4.11 ppm for two NH protons (signal d), two doublets at 7.88 and 7.95 ppm, each for four β-protons (signals b and c), and a broad signal at 9.55 ppm for two NH protons (signal a), suggesting that it has a symmetric structure. The NH assignments of the signals a and d were made on the basis of deuterium-exchange experiments with D$_2$O. At first glance, the ^{1}H NMR spectral pattern of **2a** is similar to that of **1a**, whose structure has been unambiguously determined to be a planar rectangular shape,[11,14] and hence might be interpreted in terms of a rectangular conformation analogous to that of **1a** by assigning signals e and d as the inner β- and NH-protons, respectively, signals b and c as the outer β-protons, and signal a as the outer NH-protons. Given the planar rectangular conformation, this assignment leads to the interpretation that [28]hexaphyrin **2a** exhibits a moderate diatropic ring current, since the inner protons are shielded and the outer ones are deshielded. This interpretation, however, is hard to accept, since the postulated rectangular conformation with a 28 π-electron conjugated network must lead to antiaromaticity according to the Hückel rule. Actually, the conformationally rigid systems **5** and **6**, in which one or two Au(III) ions help to strongly maintain the planar rectangular structures, feature large paratropic ring currents, as predicted by the Hückel rule.[15] In addition, the NICS value, a quantitative measure of aromaticity that was proposed by Schleyer,[16] was calculated to be large and positive (+34.5 ppm) for the planar rectangular conformation of **2a**. In sharp contrast to this

prediction, the ^{1}H NMR spectrum of **2a** shows no features indicative of a paratropic ring current arising from antiaromaticity and hence poses a question concerning the actual conformation of **2a** in solution.

One possible explanation for the strange ^{1}H NMR spectrum of **2a** is the invocation of a rapid interconversion among twisted Möbius conformations that should be aromatic (given their cyclic, conjugated, 28 π-electron structures) and thus display diatropic ring currents. In addition, the observed moderate diatropic ring current may indicate a contribution from another conformer (such as a planar rectangular conformation with antiaromatic character) that mitigates the effects of the diatropic ring current from the Möbius conformers (Scheme 2). When these conformational interconversions are fast on the ^{1}H NMR time scale, we observe an averaged ^{1}H NMR spectrum of a mixture of such isomers. In the postulated twisted Möbius conformations, all of the pyrroles are expected to be nonequivalent, and thus, the 12 pyrrolic β-protons, the 6 meso carbon atoms, and the 30 fluorine atoms in the *meso*-pentafluorophenyl substituents should be different in the ^{1}H, ^{13}C, and ^{19}F NMR spectra, respectively. In addition, the 12 β-protons should be observed in either shielded or deshielded fields, depending upon their locations (either inside or outside of the global ring current,

(10) (a) Jasat, A.; Dolphin, D. *Chem. Rev.* **1997**, *97*, 2267–2340. (b) Lash, T. D. *Angew. Chem., Int. Ed.* **2000**, *39*, 1763–1767. (c) Furuta, H.; Maeda, H.; Osuka, A. *Chem. Commun.* **2002**, 1795–1804. (d) Sessler, J. L.; Seidel, D. *Angew. Chem., Int. Ed.* **2003**, *42*, 5134–5157. (e) Chandrashekar, T. K.; Venkatraman, S. *Acc. Chem. Res.* **2003**, *36*, 676–691.

(11) (a) Shin, J.-Y.; Furuta, H.; Yoza, K.; Igarashi, S.; Osuka, A. *J. Am. Chem. Soc.* **2001**, *123*, 7190–7191. (b) Taniguchi, R.; Shimizu, S.; Suzuki, M.; Shin, J.-Y.; Furuta, H.; Osuka, A. *Tetrahedron Lett.* **2003**, *44*, 2502–2507. (c) Suzuki, M.; Osuka, A. *Org. Lett.* **2003**, *5*, 3943–3946.

(12) (a) Tanaka, Y.; Saito, S.; Mori, S.; Aratani, N.; Shinokubo, H.; Shibata, N.; Higuchi, Y.; Yoon, Z. S.; Kim, K. S.; Noh, S. B.; Park, J. K.; Kim, D.; Osuka, A. *Angew. Chem., Int. Ed.* **2008**, *47*, 681–684. (b) Jux, N. *Angew. Chem., Int. Ed.* **2008**, *47*, 2543–2546.

(13) Park, J. K.; Yoon, Z. S.; Yoon, M.-C.; Kim, K. S.; Mori, S.; Shin, J.-Y.; Osuka, A.; Kim, D. *J. Am. Chem. Soc.* **2008**, *130*, 1824–1825.

(14) Neves, M. G. P. M. S.; Martins, R. M.; Tomé, A. C.; Silvestre, A. J. D.; Silva, A. M. S.; Félix, V.; Drew, M. G. B.; Cavaleiro, J. A. S. *Chem. Commun.* **1999**, 385–386.

(15) (a) Mori, S.; Osuka, A. *J. Am. Chem. Soc.* **2005**, *127*, 8030–8031. (b) Mori, S.; Kim, K. S.; Yoon, Z. S.; Noh, S. B.; Kim, D.; Osuka, A. *J. Am. Chem. Soc.* **2007**, *129*, 11344–11345.

(16) (a) Schleyer, P. v. R.; Maerker, C.; Dransfeld, A.; Jiao, H.; Hommes, N. J. R. v. E. *J. Am. Chem. Soc.* **1996**, *118*, 6317–6318. (b) Schleyer, P. v. R.; Jiao, H.; Hommes, N. J. R. v. E.; Malkin, V. G.; Malkina, O. L. *J. Am. Chem. Soc.* **1997**, *119*, 12669–12670. (c) Chen, Z.; Wannere, C. S.; Corminboeuf, C.; Puchta, R.; Schleyer, P. v. R *Chem. Rev.* **2005**, *105*, 3842–3888.
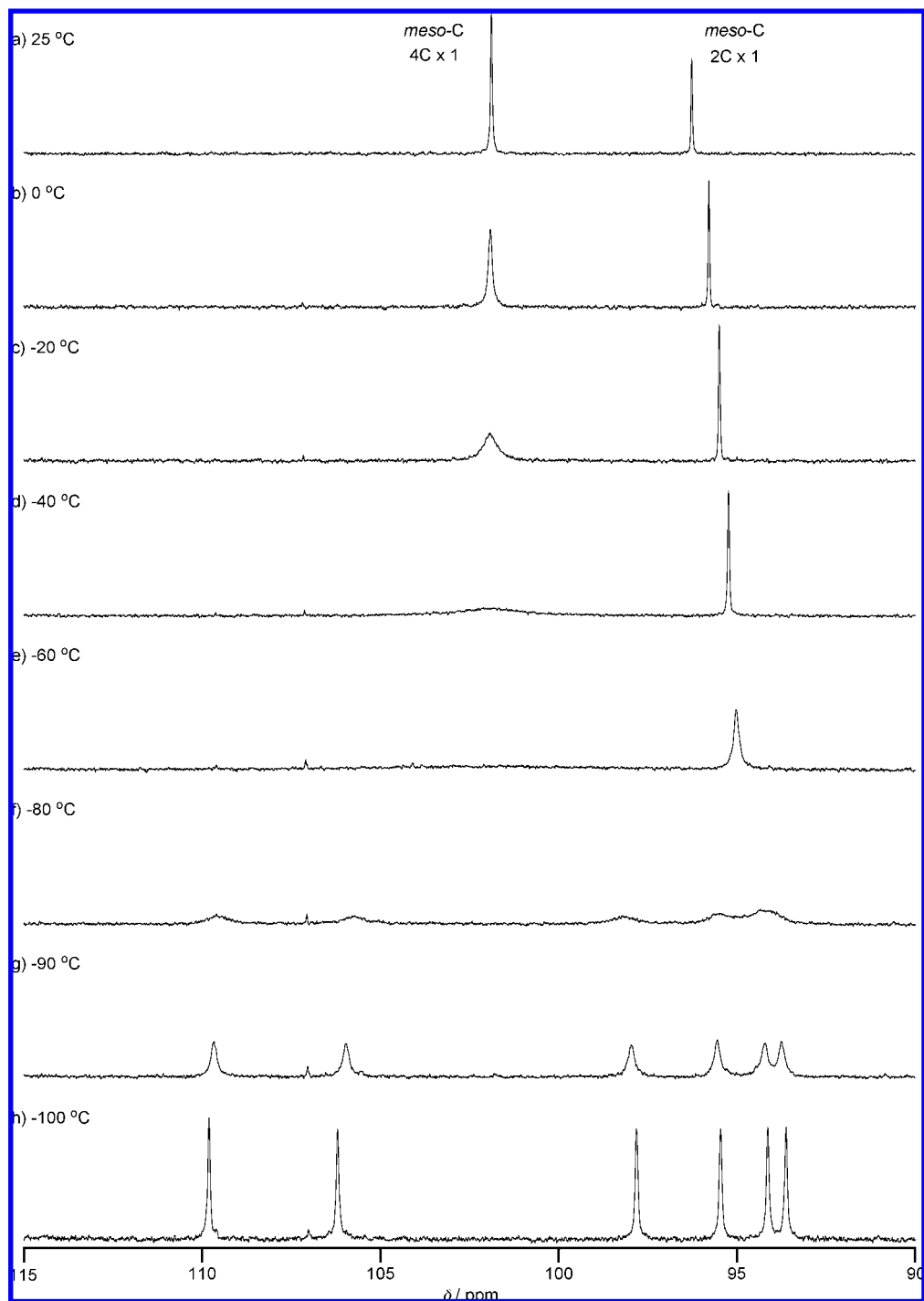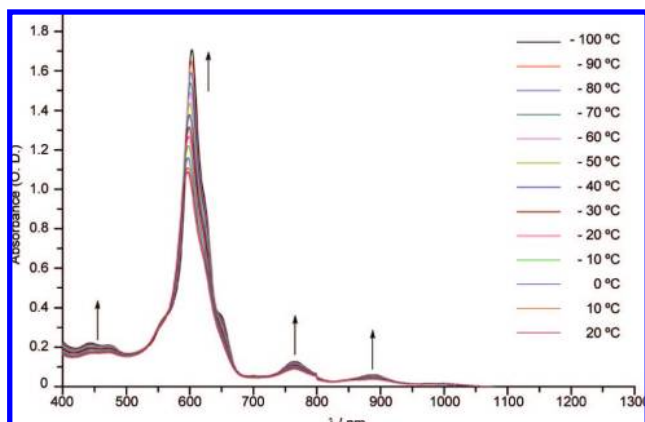
Figure 3. Variable-temperature ^{13}C NMR spectra of *meso*-^{13}C-enriched **2a** in THF-d_8 from 25 to −100 °C.

respectively), provided that such twisted Möbius molecules exhibit a measureable diatropic ring current.

We thus examined the variable-temperature ^{1}H, ^{13}C, and ^{19}F NMR spectra of **1a** and **2a**. The NMR spectra of **1a** were practically temperature-independent (see the Supporting Information). In sharp contrast, as the temperature decreased, the ^{1}H NMR spectrum of **2a** actually changed as shown in Figure 2. Initially, the peaks broadened, and this continued as the temperature decreased to −80 °C; by −100 °C, the peaks sharpened, exhibiting an interesting distribution of the β-proton signals: eight (b′ and c′) appeared in a relatively deshielded region (8.55−7.68 ppm), two (e′) at 5.08 and 4.93 ppm, and

two (e′) at −0.48 and −1.66 ppm. These spectral data thus show a large difference in the chemical shifts of the inner and outer pyrrolic β-protons, indicating a distinct diatropic ring current. These features, taken together a 28 π-electron circuit, can be explained in terms of Möbius aromaticity by postulating a twisted, one-sided macrocyclic structure.

The variable-temperature ^{13}C NMR spectra of *meso*-^{13}C-enriched **2a** were also consistent with the postulated dynamic conformational interconversion. At 25 °C, only two peaks were observed at 96.3 and 101.9 ppm (Figure 3a). This simplicity might indicate a symmetric planar rectangular conformation but instead should be interpreted in terms of the dynamic confor-

Figure 4. Variable-temperature UV−vis spectra of **2a** in THF from 20 to −100 °C.
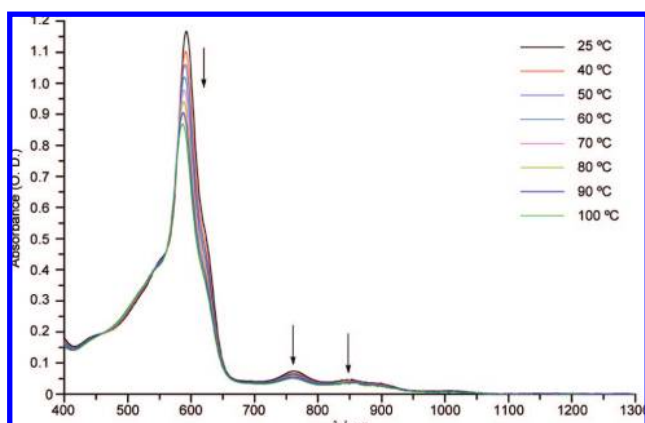
Figure 5. Variable-temperature UV−vis spectra of **2a** in toluene from 25 to 100 °C.

mational interconversion among possible twisted Möbius conformations, since the spectrum became broadened as the temperature decreased to −80 °C and then sharpened by −100 °C, displaying six peaks at 93.6, 94.1, 95.5, 97.8, 106.2, and 109.8 ppm (Figure 3). This spectrum is in accord with the Möbius structure, since such a structure has no symmetry and thus all of the meso carbons should be nonequivalent. These data again indicate that low-symmetry conformations are the most stable for **2a**. Variable-temperature ^{19}F NMR measurements on **2a** exhibited a simple spectrum at 25 °C whose peaks first broadened and then sharpened as the temperature decreased to −100 °C (Figure S3-9 in the Supporting Information); these results also support the conclusion that a dynamic conformational interconversion existing at 25 °C becomes frozen at low temperature. The ^{1}H, ^{13}C, and ^{19}F NMR spectral data consistently indicated a coalescence temperature of approximately −80 °C for **2a**.

We also examined the influence of an increase in temperature on the ^{1}H NMR spectrum of **2a** in 1,1,2,2,-tetrachloroethane-d_2 (Figure S3-8 in the Supporting Information). The variable-temperature ^{1}H NMR spectral data in the range 25−140 °C indicated a continuous decrease in the difference between the chemical shifts of the outer and inner β-protons and hence a continuous decrease in average ring current with increasing temperature. These data can be explained by invoking an increasing contribution from conformers that have nonaromatic or antiaromatic characters. This will be discussed in detail below.

We then examined the variable-temperature ^{1}H NMR and ^{19}F NMR spectra of **2b−f** and found that all of these [28]hexaphyrins exhibited temperature-dependent spectra similar to those of **2a** with coalescence temperatures of approximately −80 °C. These data strongly support the view that all of these *meso*-aryl-substituted [28]hexaphyrins(1.1.1.1.1.1) rapidly interconvert among Möbius aromatic conformations at room temperature and that such conformational dynamics are almost frozen at low temperature. At −100 °C, [28]hexaphyrin molecules prefer to avoid a planar conformation that gives rise to antiaromatic characters and settle in a nonplanar twisted Möbius geometry, probably in order to achieve energetic stabilization. It should be noted that this is the first Möbius aromatic molecular system consisting of free-base expanded porphyrins without the assistance of metal coordination, although low temperatures (−100 °C) are needed to freeze such structures on the NMR time scale.

Temperature-Dependent Absorption Spectra. The absorption spectrum of **2a** was examined as a function of temperature from 20 to −100 °C in THF (Figure 4) and from 25 to 100 °C in toluene (Figure 5). At 20 °C, **2a** exhibits a Soret-like absorption band at 596 nm and Q-band-like features at 764, 847, 892, and 1006 nm in THF; in toluene, these bands appear at 591 nm and at 763, 849, 896, and 1009 nm, respectively. The absorption spectra of **2a**, which are similar to that of **1a** with a slight broadening, seem to indicate aromatic character for **2a**. As the temperature was decreased (Figure 4), the absorption spectrum of **2a** changed gradually but distinctly: the Soret-like band became slightly red-shifted and more intense, and a shoulder appeared at 650 nm; the Q-band-like bands were also slightly more intense. The effects of an increase in temperature were also examined in toluene. As the temperature increased (Figure 5), the Soret band of **2a** became slightly broadened and blue-shifted and its intensity diminished. It is noteworthy that the intensity of the Q-band-like feature of **2a** also decreased with increasing temperature. The other [28]hexaphyrins(1.1.1.1.1.1) **2b−e** exhibited essentially the same spectral changes with an increase in temperature. These spectral changes indicate that decreasing the temperature caused an increase in aromatic character.

Single-Crystal X-ray Diffraction Studies. The solid-state structure of [26]hexaphyrin **1a** is a planar rectangular shape, and its aromaticity can be interpreted in terms of the Hückel rule.[14] It has been shown without exception to date that [26]hexaphyrins bearing 2,6-disubstituted aryl meso substituents all adopt essentially the same rectangular structures. Actually, the planar rectangular structures of **1c** and **1d** have been determined for the first time in the present work (Figures S4-1 and S4-3, respectively, in the Supporting Information). In sharp contrast, the solid-state structure of [28]hexaphyrin **2a** has remained elusive so far. A rare related example is the planar rectangular structure revealed for hexakis(4-isopropylamino-2,3,5,6-tetrafluorophenyl)-substituted [28]hexaphyrin.[17] In the present work, extensive efforts to obtain single crystals of the [28]hexaphyrins **2** were made in order to obtain more convincing solid-state evidence for their observed aromatic characters in solution. After repeated attempts, X-ray-quality single crystals of **2a** were first obtained by slow evaporation of a solution of **2a** dissolved in a ternary solvent system of dimethyl sulfoxide (DMSO), methanol, and water. Contrary to our conjecture that **2a** has a twisted Möbius topology, the single-crystal X-ray

(17) Suzuki, M.; Shimizu, S.; Shin, J.-Y.; Osuka, A. *Tetrahedron Lett.* **2003**, *44*, 4597–4601.
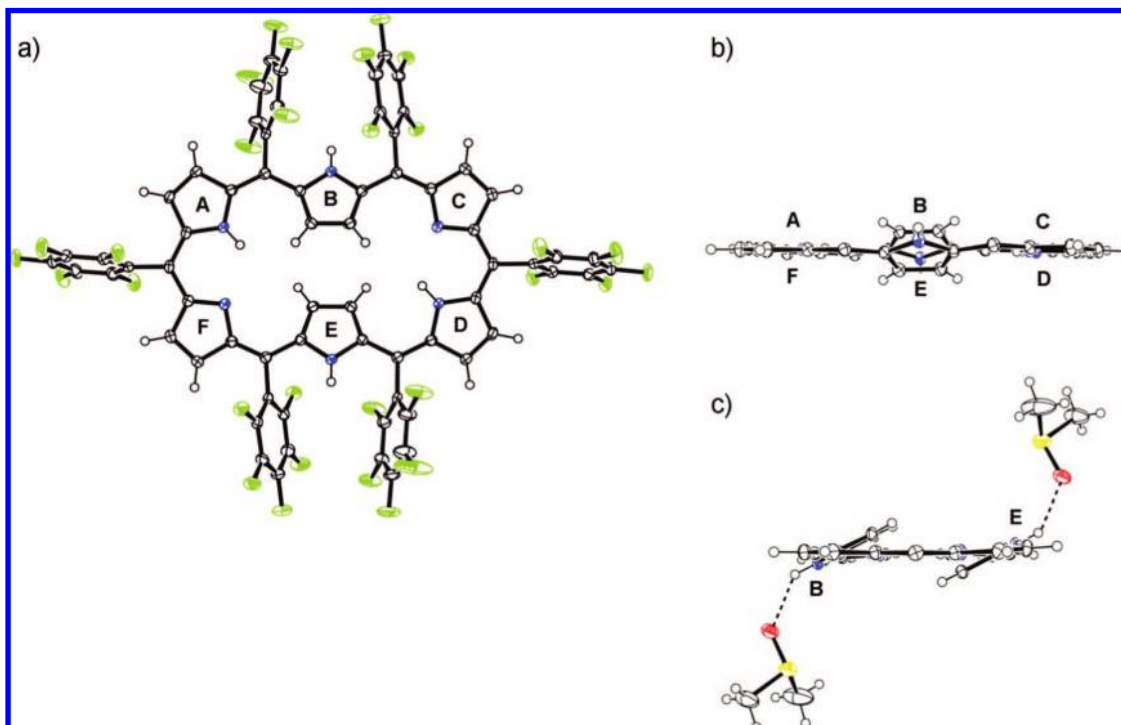
Figure 6. X-ray structure of **2a** obtained from DMSO/methanol/H$_2$O: (a) top view; (b) side view; (c) side view including the hydrogen-bonded DMSO molecules. The thermal ellipsoids are scaled to the 50% probability level. In the side views, the *meso*-aryl substituents have been omitted for clarity.
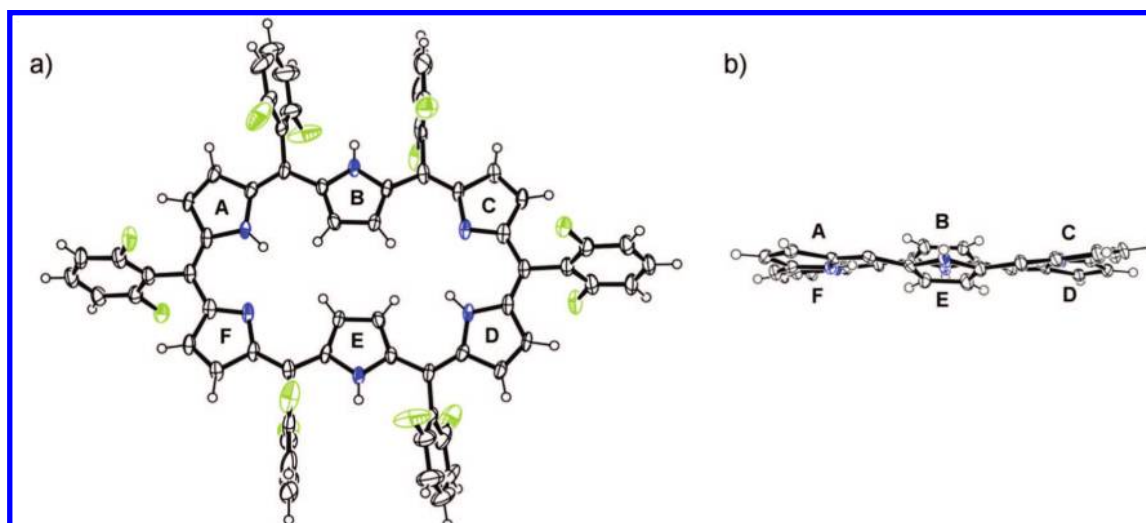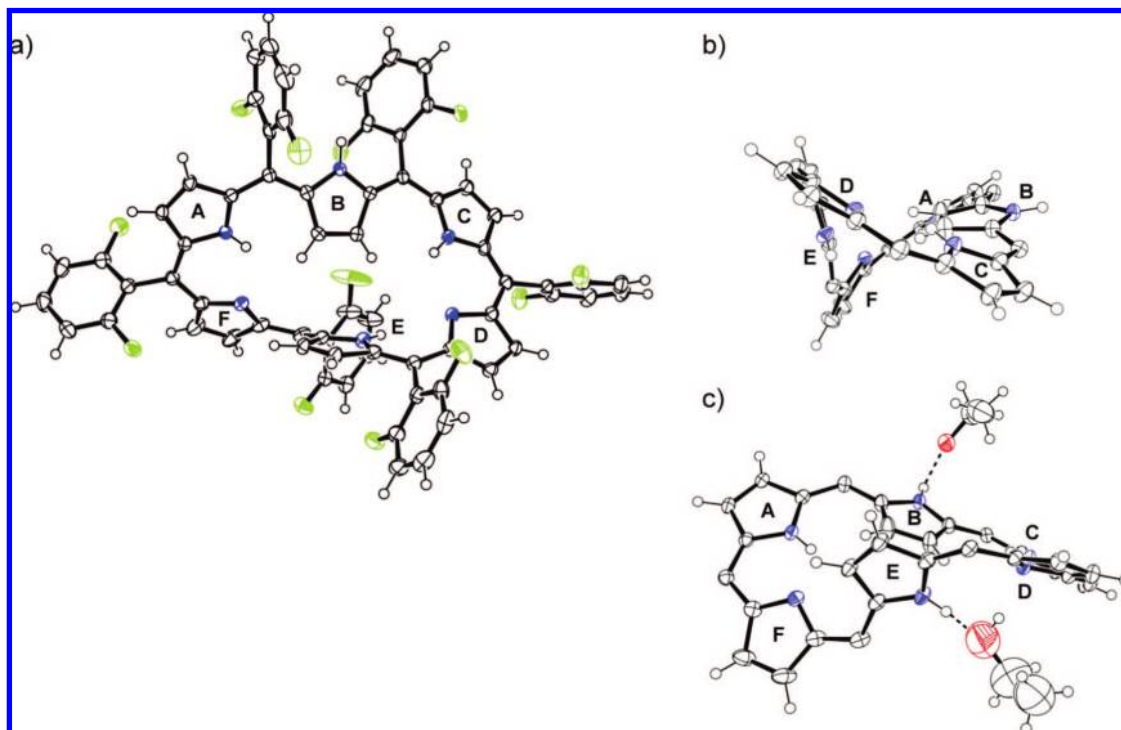

Figure 7. X-ray structure of **2b** obtained from CHCl$_3$/*n*-heptane: (a) top view; (b) side view. The thermal ellipsoids are scaled to the 50% probability level. In the side view, the *meso*-aryl substituents have been omitted for clarity.

diffraction analysis of these crystals revealed a planar rectangular structure (Figure 6) roughly similar to that of **1a**. The mean plane deviation is quite small (0.127 Å); the two inverted pyrrole rings are tilted by 26.7° with respect to the mean plane, and their outward-pointing NH protons are hydrogen-bonded to two solvent DMSO molecules, one above and one below the macrocyclic plane. This planar solid-state structure seems to arise from its favorable crystal packing, in which face-to-face, parallel, offset dimeric units are arranged along one direction and other dimeric units are arranged along a different direction in an interpenetrating manner (Figure S4-7 in the Supporting Information). Importantly, these results indicate that the planar rectangular conformation is also a stable form that can exist to some extent under certain conditions (such as in the solid state)

and thus possibly in solution. A similar planar rectangular structure was found for single crystals of **2d** that were obtained by slow vapor diffusion of *n*-heptane into a CH$_2$Cl$_2$ solution of **2d** (Figure S4-4 in the Supporting Information).

In the meantime, we found that [28]hexaphyrin **2b** provided two different crystal structures, a planar rectangular conformation and a twisted conformation, depending on the solvents used for crystallization. Slow vapor diffusion of *n*-heptane into a solution of **2b** in CHCl$_3$ yielded single crystals that provided a planar rectangular structure with a mean plane deviation of 0.203 Å (Figure 7), similar to those of **2a** and **2d**. On the contrary, slow vapor diffusion of ethanol into a solution of **2b** in 1,2-dichloroethane gave different single crystals that were found to have a distorted structure of Möbius topology (Figure 8) in which two

Figure 8. X-ray structure of **2b** obtained from 1,2-dichloroethane/ethanol: (a) top view; (b) side view; (c) side view including the hydrogen-bonded ethanol molecules. The thermal ellipsoids are scaled to the 50% probability level. In the side views, the *meso*-aryl substituents have been omitted for clarity.
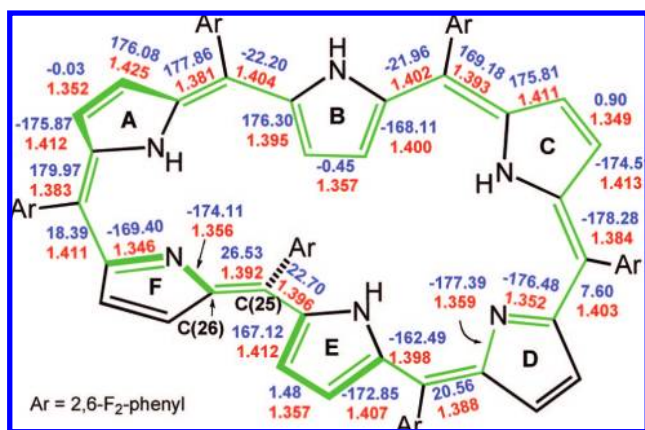

Figure 9. Detailed structural data for the Möbius structure of **2b** from Figure 8. The conjugated 28 π-electron circuit is indicated in green, along which bond lengths (Å) are indicated in red and dihedral angles (deg) in blue.

ethanol molecules are hydrogen-bonded with the outward-pointing NH protons of pyrroles B and E. Detailed structural data, including bond distances and dihedral angles, are summarized in Figure 9. The overall electronic system can be delineated as a conjugated cyclic network containing a 28 π-electron periphery. Significantly, even at the most distorted position along the conjugated chain, C(25)−C(26), the dihedral angle is only 26.5°, which is still favorable for the overall conjugation. This feature is different from those observed for Pd(II) complexes of expanded porphyrins,[12a] in which the metal coordination helps rigidify the twisted structure but enforces relatively planar local coordination structures [square planar in the case of Pd(II)], resulting in a considerably large dihedral angle. In the Möbius structure of **2b**, the large strain arising from the molecular twist is dissipated across the whole macrocyclic ring system, probably as a consequence of the conformational flexibility. When we as-

sumed a similar twisted Möbius structure for **2a**, it became possible to assign the e′ signals at −2.25 and −1.47 ppm in the ^{1}H NMR spectrum recorded at −100 °C (Figure 2h) to the β-protons of inverted pyrrole B and the e′ signals at 4.90 and 4.82 ppm to those of pyrrole E (for ring labels, see Figure 8).

As another examples, we obtained single crystals of **2c** and **2f** by slow vapor diffusion of hexane into a CHCl₃ solution and *n*-heptane into a THF solution, respectively. The crystal structures of **2c** and **2f** (Figures S4-2 and S4-5, respectively, in the Supporting Information) were found to be Möbius structures similar to that of **2b**. The large strain associated with the molecular twist is dissipated nicely across the whole molecule, assuring effective π conjugation over the macrocycle. In the case of **2f**, the crystal structure indicated a single regioisomer, but the ^{1}H NMR spectrum at −100 °C (Figure S3-21h in the Supporting Information) revealed the presence of a minor regioisomer (~20%), reflecting the alternating meso substitution pattern. These results indicate that **2c** and **2f** settle at their most stable twisted Möbius conformations at −100 °C, at which the possible conformational changes are practically frozen.

The Möbius solid-state structures observed for **2b**, **2c**, and **2f** are significant because they confirm that the aromatic characters actually arise from their 28 π-electron circuits lying on single-sided Möbius strips. The experimental fact that two different crystal structures were obtained for **2b** is also important, as it indicates not only that the energy difference between these two structures is small but also that differences in solvents such as polarity or hydrogen-bonding ability can affect the crystal structure, which should also depend on the crystal packing. Therefore, it is plausible to conclude that there is some contribution from the planar rectangular conformer or even from other conformers of [28]hexaphyrins in solution. Importantly, however, it is also reasonable to conclude that the Möbius conformations are the most energetically stable, since they are predominant at low temperatures.
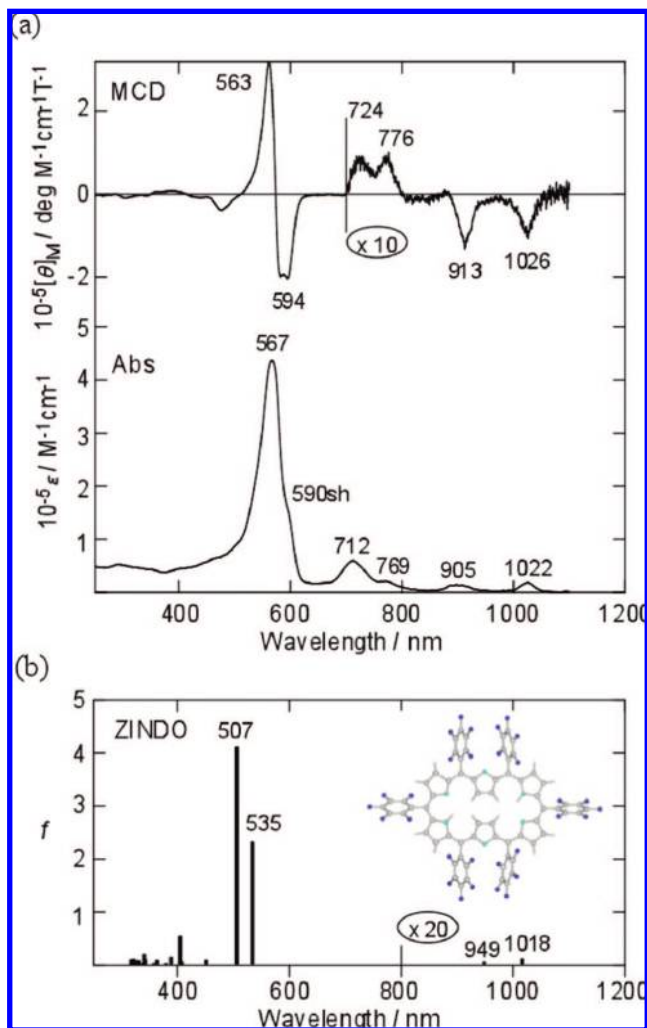
Figure 10. (a) Experimental MCD and absorption spectra of **1a** measured in CH_2Cl_2 at room temperature. (b) Calculated absorption spectrum of Hückel-type **1a** obtained using the ZINDO/S method. The inset shows the B3LYP-optimized structure used in the ZINDO/S calculations.

The harmonic-oscillator model for aromaticity (HOMA) values obtained from the X-ray diffraction data provide important information about the extent of effective electronic delocalization.[18] The solid-state planar structure of **2a** gives a HOMA value of 0.450, which is smaller than the value of 0.647 for the [26]hexaphyrin **1a**, indicating less effective conjugation in the planar form of **2a**. On the other hand, significantly large HOMA values were commonly observed for the Möbius structures of **2b** (0.85), **2c** (0.69), and **2f** (0.71). Therefore, it can be concluded that the overlap of π orbitals in [28]hexaphyrin is more effective in a twisted Möbius topology than in a planar rectangular shape.

MCD Spectroscopy. Magnetic circular dichroism (MCD) spectroscopy has long proven to be an important technique for determining the electronic and magnetic properties and coordination structures of organic and inorganic systems.[19] Analysis of MCD spectra often facilitates identification of the main electronic transitions in instances where such identification is not possible on the basis of an analysis of the UV−visible absorption spectra alone. In the case of porphyrinoid systems such as porphyrins,[20] chlorins,[21] azaporphyrins,[22] and porphycenes,[23] MCD spectroscopy has provided the key information required for definitive band assignment and characterization of the electronic excited states. In recent years, the electronic structures of expanded porphyrins such as texaphyrins,[24] isosmaragdyrins,[25] sapphyrins,[26] and cyclo[n]pyrroles[27] have also been analyzed using MCD spectroscopy. We measured the MCD spectra of a range of different hexaphyrins in order to determine the relationship between Hückel- and Möbius-type aromaticities and the electronic structures.
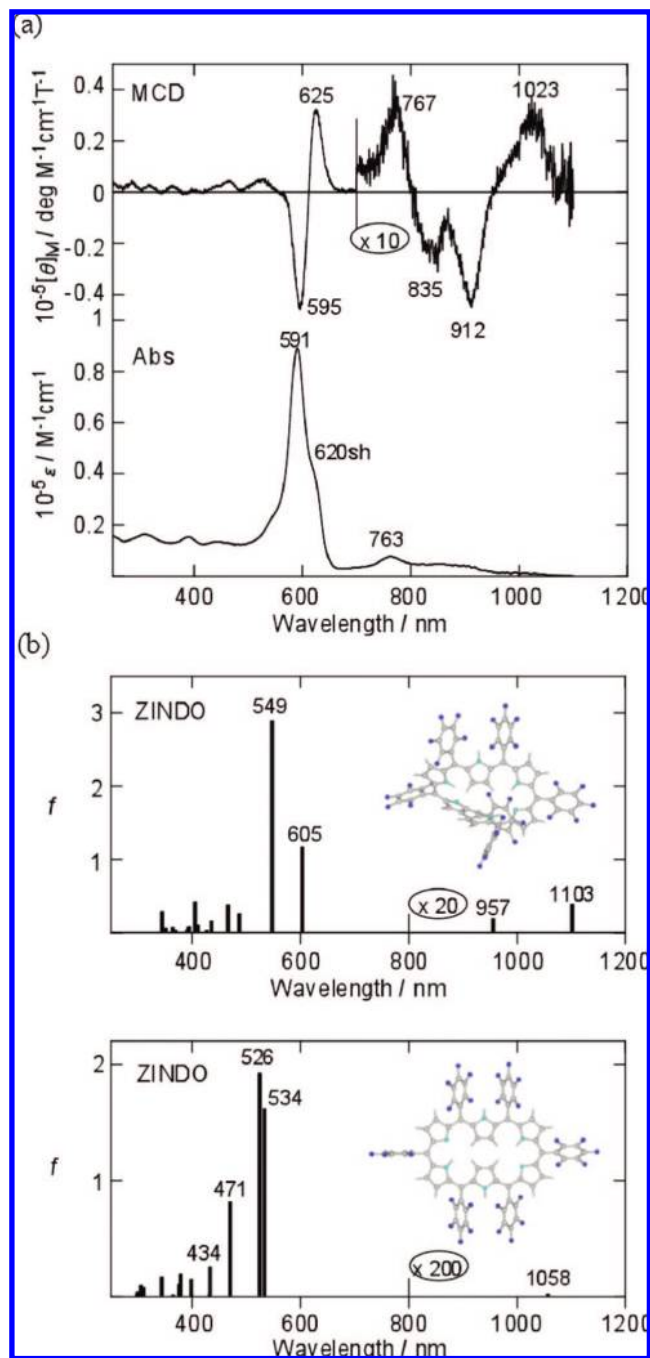
Figure 10a shows the electronic absorption and MCD spectra of [26]hexaphyrin **1a** measured in CH_2Cl_2 at room temperature. **1a** exhibits four weak absorption bands (1022, 905, 769, and 712 nm) and an intense absorption band (567 nm) with a shoulder on the longer-wavelength side (∼590 nm). In the MCD spectrum of **1a**, four Faraday *B* terms having a −,−,+,+ sign sequence with increasing energy were observed for the four weak absorption bands. Intense positive and negative MCD signals corresponding to the 567 nm absorption and its shoulder, respectively, were detected, indicating that there are at least two different electronic transitions in the 550−600 nm region. The overall MCD pattern of **1a** appears to be essentially similar to those of conventional free-base porphyrins.[28] We calculated the absorption spectrum of Hückel-type **1a** using the ZINDO/S method in order to make definitive band assignments. As shown in Figure 10b, the calculated results agreed well with the experimental observations. Two closely lying transitions were predicted at 507 and 535 nm, corresponding to the observed 567 nm absorption band and 590 nm shoulder band, respectively. These transitions are polarized along the long and short molecular axes, respectively. This can account for the strongly coupled Faraday *B* terms observed experimentally, since according to theory, mutually perpendicular transitions in a narrow energy region give strongly coupled Faraday *B* terms.[19] With respect to the longer-wavelength region, two very weak electronic transitions were calculated at 949 and 1018 nm. Since **1a** has four weak absorption bands in the near-IR region, it was reasonable to assign the observed 769 and 1022 nm transitions to an electronic origin and the 712 and 905 nm bands as vibronic bands, as is the case of normal free-base porphyrins.[28] It is noted that these four excitations consist of electronic transitions involving the four π frontier molecular orbitals (MOs) HOMO−1, HOMO, LUMO, and LUMO+1 (see Table 1). In Platt

Table 1. Calculated Excitation Wavelengths (λ), Oscillator Strengths (*f*), and Compositions of Electronic Transitions in Hückel-Type **1a** and Möbius-Type **2a** Obtained Using ZINDO/S Calculations

compound	λ(nm)	assign.	*f*	composition (%)[a]
1a (Hückel)	1018	L_I	0.006	H → L (37.5); H−1 → L+1 (26.1); H−1 → L (16.1); H → L +1(15.6)
	949	L_{II}	0.003	H → L+1 (32.4); H−1 → L (30.3); H → L (17.1); H−1 → L+1 (14.0)
	535	B_I	2.319	H−1 → L+1 (38.7); H → L (28.3); H → L+1 (11.1); H−1 → L (10.0)
	507	B_{II}	4.112	H−1 → L (31.8); H → L+1 (30.1); H−1→ L+1 (11.9); H → L (9.3)
2a (Möbius)	1103	L_I	0.019	H → L (55.1); H−1 → L+1 (39.2)
	957	L_{II}	0.009	H−1 → L (57.8); H → L+1 (35.2)
	605	B_I	1.169	H → L+1 (48.7); H−1 → L (27.1)
	549	B_{II}	2.892	H−1 → L+1 (48.4); H → L (36.0)

[a] H = HOMO, L = LUMO.

nomenclature,[29] the two lower-energy quasi-allowed transitions and the two higher-energy strongly allowed transitions are labeled as the L and B bands, respectively. Since it is customary to refer to the two L bands of porphyrins as the Q bands and the two B bands as the Soret bands, we can also use the labels Q and Soret, respectively, to refer to the L and B transitions of **1a**.

The electronic absorption and MCD spectra of [28]hexaphyrin **2a** are shown in Figure 11a. As mentioned earlier, **2a** exhibits a red-shifted visible band at 591 nm with a shoulder at ~620 nm, and the long-wavelength absorption bands observed between 700 and 1100 nm are weak and broad. We found that the MCD sign pattern for the intense visible band of **2a** was inverted compared with that of **1a**. Thus, an intense MCD peak and trough were observed at 625 and 595 nm, respectively. In the near-IR region, four MCD signals (1023, 912, 835, and 767 nm) were clearly resolved, indicating the presence of four different electronic transitions. The MCD sign corresponding to the lowest-energy transition was positive, in contrast to the negative MCD for the corresponding peak of **1a**. Figure 11b gives the calculated absorption spectra of two types of **2a**. One can see clearly that the observed spectral patterns were well-reproduced by the Möbius structure. The results calculated on the basis of the Hückel structure did not predict the red-shifted visible band or the four near-IR bands. Two weak transitions in the near-IR region (957 and 1103 nm) were predicted for the Möbius conformation, so the MCD signals at 835 and 1023 nm were assigned to have a purely electronic origin while the 767 and 912 nm signals are vibronic bands. As shown in Table 1, the four electronic absorption bands could be described in terms of the four key π frontier MOs of Möbius **2a**. We therefore applied the Platt nomenclature[29] to assign the absorption bands of Möbius **2a**. The polarization directions of the 549 and 605 nm transitions for Möbius **2a** are almost parallel to the long and short molecular axes, respectively.

Figure 12 illustrates the MOs of Möbius [28]hexaphyrin, Hückel [26]hexaphyrin, and Hückel [28]hexaphyrin calculated using density functional theory (DFT) at the B3LYP/6-31G*

Figure 11. (a) Experimental MCD and absorption spectra of **2a** measured in CH_2Cl_2 at room temperature. (b) Calculated absorption spectra of (top) Möbius-type **2a** and (bottom) Hückel-type **2a** obtained using the ZINDO/S method. The insets show the B3LYP-optimized structures used in the ZINDO/S calculations.

level.[30] At first glance, a similarity is seen between Möbius [28]hexaphyrin and Hückel [26]hexaphyrin with respect to the near degeneracy of their MOs, which is characteristic of general aromatic compounds. The degenerate MOs account well for the porphyrin-like absorption spectra of **1** and **2**, which consist of Soret-like and the Q-band-like bands. In sharp contrast, no degeneracy was observed in the case of Hückel [28]hexaphyrin.

(18) Krygowski, T. M. *J. Chem. Inf. Comput. Sci.* **1993**, *33*, 70–78, HOMA values are a quantitative measure of bond-length equalization for π-electron systems. HOMA = 0 for the Kekulé structure of an aromatic system, and HOMA = 1 for the system with all bonds equal to the optimal value, such as in benzene.

(19) (a) Mason, W. R. *A Practical Guide to Magnetic Circular Dichroism Spectroscopy*; John Wiley & Sons Inc.: Hoboken, NJ, 2007. (b) Rodger, A.; Nordén, B. *Circular Dichroism and Linear Dichroism*; Oxford University Press: Oxford, U.K., 1997.

(20) (a) Michl, J. *J. Am. Chem. Soc.* **1978**, *100*, 6801–6811. (b) Michl, J. *J. Am. Chem. Soc.* **1978**, *100*, 6812–6818. (c) Mack, J.; Asano, Y.; Kobayashi, N.; Stillman, M. J. *J. Am. Chem. Soc.* **2005**, *127*, 17697–17711.

(21) (a) Keegan, J. D.; Stolzenberg, A. M.; Lu, Y.-C.; Linder, R. E.; Barth, G.; Moscowitz, A.; Bunnenberg, E.; Djerassi, C. *J. Am. Chem. Soc.* **1982**, *104*, 4305–4317. (b) Keegan, J. D.; Stolzenberg, A. M.; Lu, Y.-C.; Linder, R. E.; Barth, G.; Moscowitz, A.; Bunnenberg, E.; Djerassi, C. *J. Am. Chem. Soc.* **1982**, *104*, 4317–4329.

(22) Mack, J.; Stillman, M. J. *Coord. Chem. Rev.* **2001**, *219−221*, 993–1032.

(23) Waluk, J.; Müller, M.; Swiderek, P.; Köcher, M.; Vogel, E.; Hohlneicher, G.; Michl, J. *J. Am. Chem. Soc.* **1991**, *113*, 5511–5527.

(24) Waluk, J.; Hemmi, G.; Sessler, J. L.; Michl, J. *J. Org. Chem.* **1991**, *56*, 2735–2742.

(25) Gorski, A.; Lament, B.; Davis, J. M.; Sessler, J. L; Waluk, J. *J. Phys. Chem. A* **2001**, *105*, 4992–4999.

(26) Lament, B.; Rachlewicz, K.; Latos-Grażyński, L.; Waluk, J. *ChemPhysChem* **2002**, *3*, 849–855.

(27) Gorski, A.; Köhler, T.; Seidel, D.; Lee, J. T.; Orzanowska, G.; Sessler, J. L.; Waluk, J. *Chem.−Eur. J.* **2005**, *11*, 4179–4184.

(28) Gouterman, M. In *The Porphyrins, Vol. III: Physical Chemistry, Part A*; Dolphin, D., Ed.; Academic Press: New York, 1978.

(29) Platt, J. R. *J. Chem. Phys.* **1949**, *17*, 484–495.

(30) (a) Becke, A. D. *Phys. Rev. A* **1988**, *38*, 3098–3100. (b) Lee, C.; Yang, W.; Parr, R. G. *Phys. Rev. B* **1988**, *37*, 785–789. (c) Theoretical calculations were performed with the Gaussian 03 package: Frisch, M. J.; et al. *Gaussian 03*, revision B.05; Gaussian, Inc.: Wallingford, CT, 2004.
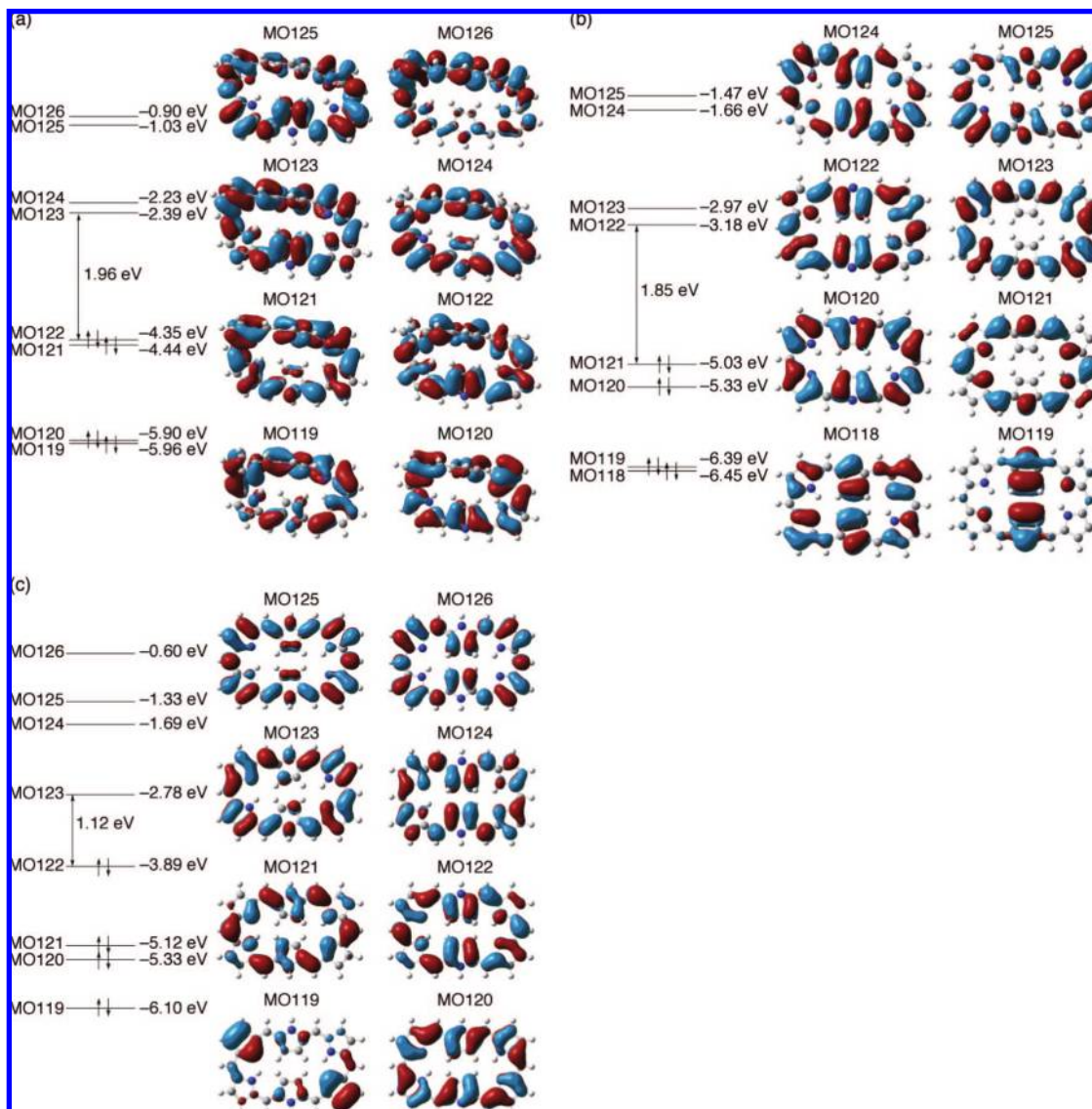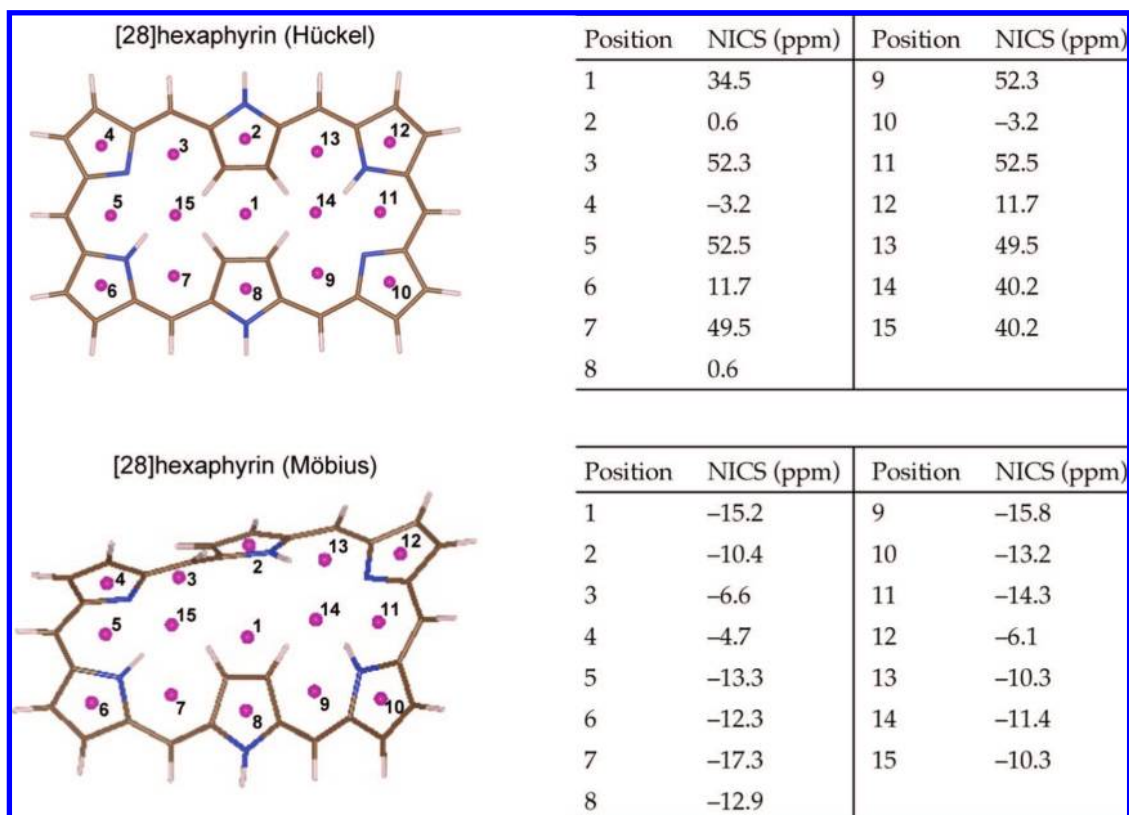
Figure 12. Molecular orbitals (B3LYP/6−31G*) of (a) Möbius [28]hexaphyrin, (b) Hückel [26]hexaphyrin, and (c) Hückel [28]hexaphyrin.

The origin of the observed MCD properties of **1a** and **2a** is now further discussed in terms of an examination of their electronic structures. In the case of Hückel aromatic molecules derived from a [4n + 2]-electron perimeter, the absolute MCD signs associated with the two L and two B transitions can be deduced from the properties of the frontier MOs.[20] In particular, in the case of low-symmetry aromatic molecules whose four transitions are described within a four-orbital π-electron framework, the MCD signs are predicted by the relative sizes of the two MO energy differences ΔHOMO and ΔLUMO, which represent the differences between the absolute values of the energy of the two highest occupied MOs and between the two lowest unoccupied orbitals, respectively.[20b,21,23–26] When ΔHOMO = ΔLUMO ≠ 0, the MCD signs derive from μ^{-} contributions, and the MCD having a purely electronic origin is likely to be generally quite weak. The MCD sign pattern for this kind of system would be −,−,−,+ with increasing energy. When ΔLUMO − ΔHOMO is relatively large, μ^{+} contributions dominate, and the MCD sign pattern is governed by the sign of ΔLUMO − ΔHOMO: when this quantity is negative (i.e., when ΔHOMO > ΔLUMO), a −,+,−,+ sign sequence in order of increasing energy is predicted, whereas the inverted sequence

+,−,+,− is anticipated when ΔHOMO < ΔLUMO. We calculated the orbital-energy differences for Hückel **1a** and its unsubstituted derivative **1_H** using the DFT, Hartree-Fock (HF), and ZINDO/S methods. As shown in Table S3 in the Supporting Information, ΔHOMO > ΔLUMO for **1a** regardless of the computational level. This led to the prediction of the −,+,−,+ sign pattern for the two L and two B bands, matching the experimentally observed pattern. In the case of the parent **1_H**, ΔHOMO ≈ ΔLUMO, so the hexaphyrin skeleton itself can be classified into the soft-chromophore case.[20b]

The electronic structures of Möbius-type **2a** and the unsubstituted derivative **2_H** were found to be considerably different from those for Hückel-type **1a** and **1_H**. As shown in Table S3 and Figure S6 in the Supporting Information, ΔHOMO < ΔLUMO relationships were predicted for **2a** and **2_H**. Although no theory for the absolute MCD sign of Möbius aromatic molecules has been reported to date, the sign inversion of the ΔLUMO−ΔHOMO values of Möbius-type **2a** and **2_H** compared with those of **1a** may be correlated with the inversion of the MCD pattern observed for **2a**, since even in Möbius aromatic systems, the orbital-energy difference depends on whether the transition is an electron-dominated excitation or a hole-dominated excitation.

[28]hexaphyrin (Hückel)

Position	NICS (ppm)	Position	NICS (ppm)
1	34.5	9	52.3
2	0.6	10	−3.2
3	52.3	11	52.5
4	−3.2	12	11.7
5	52.5	13	49.5
6	11.7	14	40.2
7	49.5	15	40.2
8	0.6		

[28]hexaphyrin (Möbius)

Position	NICS (ppm)	Position	NICS (ppm)
1	−15.2	9	−15.8
2	−10.4	10	−13.2
3	−6.6	11	−14.3
4	−4.7	12	−6.1
5	−13.3	13	−10.3
6	−12.3	14	−11.4
7	−17.3	15	−10.3
8	−12.9		

Figure 13. NICS values for (top) Hückel and (bottom) Möbius [28]hexaphyrin calculated at the GIAO-B3LYP/6-31G* level.

Theoretical Calculations and Analysis of Aromaticity on the Basis of NICS Values. To evaluate aromaticity and antiaromaticity of hexaphyrins both in Möbius and Hückel topologies, we carried out DFT calculations at the B3LYP/6-31G* level based on the optimized structures. Initial geometries of the models were obtained from X-ray structures, but all of the aromatic substituents were replaced by hydrogens. NICS values of the optimized structures were obtained as a qualitative measure of aromaticity and antiaromaticity. For each model, the NICS values at the global ring center of the macrocycle as well as at the center of each pyrrole unit and each formal ring structure between adjacent pyrroles were calculated, as shown in Figure 13. Clearly, [28]hexaphyrin in the Möbius topology, for which the NICS value was calculated to be −15.2 ppm at the center of the molecule, is strongly aromatic. This value is comparable to those of [26]hexaphyrin (−16.7 ppm) and the bis[Au(III)] complex of [26]hexaphyrin (−12.5 ppm), both of which have been shown to be strongly aromatic.[15a] Consequently, the DFT calculations clearly suggested the strong aromaticity of the macrocycle, which was also obvious from the ^{1}H NMR measurements and X-ray analysis. In addition, the HOMA value for the optimized structure was calculated to be 0.71, again indicating the aromaticity of Möbius [28]hexaphyrin. This value is in good agreement with the experimental value, demonstrating the validity of the calculations. On the other hand, [28]hexaphyrin in the Hückel topology was calculated to have a considerably positive NICS value (+34.5 ppm) at the molecular center and a HOMA value of 0.51; comparison of this NICS value with that of the antiaromatic bis[Au(III)] complex of [28]hexaphyrin (37.3 ppm) reveals the strong antiaromaticity of Hückel [28]hexaphyrin.

Conclusion

In summary, *meso*-aryl-substituted [28]hexaphyrins(1.1.1.1.1.1) have been shown to exist in solution at 25 °C largely as an equilibrium of several rapidly interconverting twisted Möbius conformations with distinct aromaticities, with a small contribution from a rectangular conformation with antiaromatic character. When the temperature was decreased to −100 °C in THF, these rapid interconversions were frozen, leading to the predominant existence of a single Möbius conformation with distinct aromaticity, as revealed by the NMR measurements. The MCD data were also consistent with the Möbius structure. Furthermore, the Möbius-twisted conformations were actually confirmed by the single-crystal diffraction studies. Hence, this work has demonstrated the first example of Möbius aromatic molecules consisting of free-base expanded porphyrins without any assistance of metal chelation. These Möbius aromatic free-base expanded porphyrins constitute a nice platform for examination of various properties of Möbius aromaticity.